

## Chapter

# Using the iESP Installed on the Space Station Moving in an Irregular Gravitational Field of the Asteroids Eros and Gaspra

*Olga Starinova, Andrey Shornikov and Elizaveta Nikolaeva*

## Abstract

The gravitational field of asteroids and comets often has a complex dynamically changing shape. The study of the gravitational field of such bodies is essential for the design of missions, especially for missions involving maneuvering in close proximity, landing, and takeoff from the surface of a celestial body. This chapter deals to the problem of spacecraft's controlled motion near objects with irregular gravitational fields. We propose to use a propulsion system based on ion electro spray propulsions (iESP), which usually used to control the spacecraft's motion relative to the mass center. The chapter describes the gravitational field of an asteroid as the superposition of the fields of two rotating point masses. The proposed control laws made it possible to stabilize the orbit near the asteroid surface. We performed the simulation of motion close to two relatively well-studied asteroids Eros and Gaspra. The results of the simulation demonstrated that the using of iESP as the auxiliary propulsion systems is sufficient to control the spacecraft's motion in irregular gravitational fields.

**Keywords:** asteroid, boundary task, electric propulsion engine, gravitational potential, n-body problem, spacecraft, iESP, electro spray engine

## 1. Introduction

Over recent decades, there has been an increase in interest of the asteroids, comets, and other small celestial body studies. This is due to the changes in the research vector toward the solution of applied problems: counteraction to asteroids [1] and comet [2] hazards and development of small solar system objects with the purpose of mineral extraction [3, 4].

When designing research missions, there is a problem of the development of spacecraft control schemes in the attraction fields of complex geometric shapes bodies. The gravitational force between the elementary masses in that type of bodies is not sufficient to form the bodies in correct ellipsoidal or spheroidal form. Complex geometry creates the gravitational field of the complex configuration [1]. The spacecraft's behavior in this field is significantly different from the behavior of similar spacecraft near ellipsoidal and spheroidal bodies, the shape of which, as well as their gravitational field, can be considered correct in some approximation. The

modeling of spacecraft motion and the development of control schemes near asteroids and comets is possible only under the condition that those bodies gravitational field formalization task was solved with the prescribed accuracy. However, if we take into consideration cavities and voids in the object structure, the center of masses displacement, and the uneven distribution of density [5], it becomes difficult to solve the gravitational field formalization problem.

In addition to the high accuracy of the gravitational field model, the lightweight of the model plays a huge role in ballistic design. The task of the spacecraft motion modeling and the task of finding optimally sustainable control schemes are virtually non-solvable because of the overloaded model of gravitational potential. That is why the task is to find a balance between the accuracy of the object's potential appearance and the convergence property of the task.

The problem of finding the correct mathematical description of the gravitational fields of different shaped objects was addressed in a number of sources. For example, in the paper [6], the authors address the polygonal method of presenting the gravitational potential of asteroid 4769 Castalia as a formal model. A comparison of the proposed approach with the model of point attracting center takes place in the paper [7], where authors present a comparative analysis of the polygonal model and the model of point attracting center for the asteroid 216 Cleopatra. The paper [8] described and compared the gravitational potential presented in the form of series expanded into spherical, spheroidal, and ellipsoidal functions for Martian moons. In the paper [9], the authors address the position of equilibrium points for 23 different asteroids in their polygonal models of gravitational fields.

The drawbacks of the approaches addressed are their cumbersomeness when using in the problems of spacecraft flight dynamics and the necessity to know in advance the physical properties of the objects—geometry and mass distribution. Modeling the gravitational field of objects whose properties and structure are not known in advance within the models described is not possible.

This work analyzes the possibility of using ion electrospay propulsions to stabilize the orbit of a spacecraft that maneuvers in the gravitational field of an object of complex geometric shape using the asteroid 433 Eros and 951 Gaspra as examples. The choice of these asteroids is due to the presence of sufficient information about the gravitational fields of these bodies [10–12]. Besides, 433 Eros and 951 Gaspra are quite massive, and therefore it is impossible to ignore the uneven distribution of their gravitational field in space [12–14]. The authors used this information in [1, 15] to prove the correctness of the models used.

As a result of motion simulation, the authors developed an idea of using the iESP module for the controlled motion in the vicinity of the asteroid. Such modules are able to gain necessary thrust and exhaust velocity for the stable motion near the asteroid.

## **2. Models of an irregular gravitational field**

The chapter presents a model of the gravitational potential of asteroid 433 Eros and 951 Gaspra in terms of the applicability of the model in the problems of flight dynamics. It should be noted that the described model of motion does not require fundamental knowledge about the structure and composition of the object. The purpose of the analysis is to show that this method of describing the gravitational potential provides sufficient accuracy for subsequent flight design.

This work uses the asteroids 433 Eros and 951 Gaspra as examples cosmic bodies with irregular gravitational fields. The choices of these asteroids are explained by the shape of the asteroid, its mass and its orbit. According to [14], the physical properties and orbital characteristics asteroids are presented in **Table 1**.

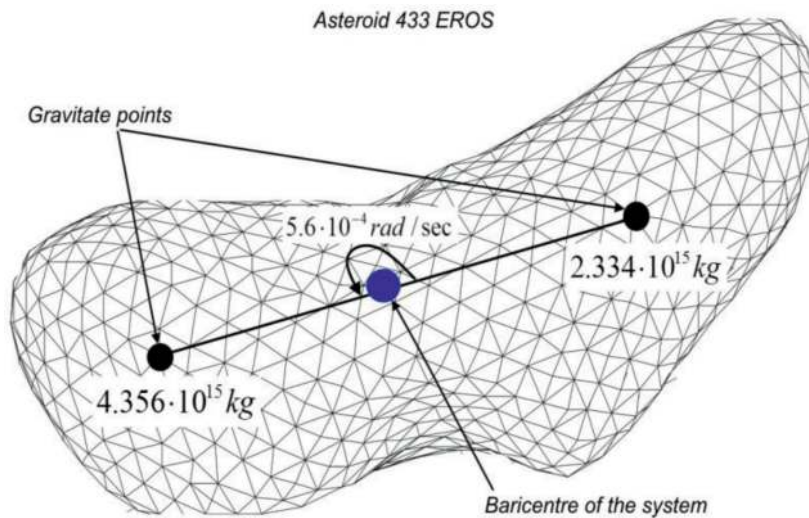


**Figure 1.**  
 Asteroid Eros 433 as a superposition of two rotation mass points.

A number of mathematical methods can be used for deriving a model of an irregular gravitational field. This chapter suggests the model of gravitational potential based on the n-body problem. Authors developed the idea of superposition of single gravitate mass points potential. The problem is to determine the necessary number of mass points and to define their locations. It is considered that two gravity points suffice for the simulation of gravitational field. It should be noted that the model under consideration assume that the asteroid's density is distributed evenly throughout the body to simplify the calculations.

In the paper [15], authors compare the barycentric form of gravitational potential and gravitational potential in spherical harmonic coefficients. It is proved that barycentric potential is accurate enough for the motion simulations.

Let  $M_1, M_2$  is masses of gravity points and  $\mathbf{r}_1 = (x_1, y_1, z_1), \mathbf{r}_2 = (x_2, y_2, z_2)$  are their vector positions (**Figure 1**). The corresponding form of the gravitational potential  $U_{x,y,z}$  for this case is taken from [16]:

Physical characteristics of the asteroids 433 Eros and 951 Gaspra		
Mass, kg	$6.69 \times 10^{15}$	$2-3 \times 10^{16}$
Density, kg/cm <sup>3</sup>	2.67	2.7
Dimensions, km	$34.4 \times 11.2 \times 11.2$	$18.2 \times 10.5 \times 8.9$
Mean diameter, km	16.84	12.2
Rotation period, hours	5.27	7.04
Orbital characteristics of the asteroids 433 Eros and 951 Gaspra		
Eccentricity	0.22263	0.17363
Major axis, a.u.	1.45796	2.20971
Perihelion argument, deg	178.79567	129.72454
Inclination of orbit, deg	10.8289	4.10220
Circulation period, days	642.989	1199.782
Longitude of ascending node, deg	304.33453	253.17193

**Table 1.**  
 Physical and orbital characteristics of the asteroids 433 Eros and 951 Gaspra.

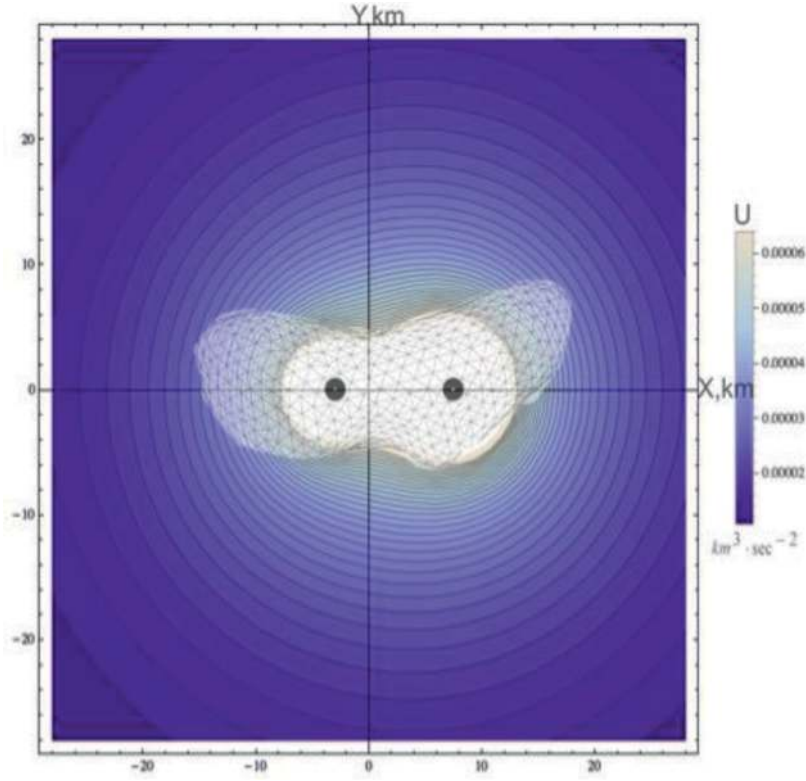


**Figure 2.**  
Gravitational force lines of the Eros.

$$U_{x,y,z} = G \cdot \sum_{i=1}^{K=2} \frac{M_i}{\sqrt{(x - x_i)^2 + (y - y_i)^2 + (z - z_i)^2}} \quad (1)$$

$$\omega = \sqrt{\frac{G(M_1 + M_2)}{d^3}} \quad (2)$$

where  $G$  is the gravitational constant;  $\mathbf{r} = (x, y, z)$  is vector of a spacecraft's position;  $\omega$  is the angular velocity of the rotating around the barycentre; and  $d$  is the distance between the mass points. Hereafter, we call the potential (1) as the barycentric potential.

For example, in [15] we have analyzed the gravitational field of the asteroid 433 Eros and have calculated the exact mass values and the distance between the gravity points by trial and errors method. The following parameters of model  $M_1 = 4.356 \cdot 10^{15}$  kg,  $M_2 = 2.334 \cdot 10^{15}$  kg,  $d = 10.8$  km, and  $\omega = 5.6 \cdot 10^{-4}$  rad/s provide a minimum error in comparison with the gravitational potential described in the paper [11]. **Figure 2** shows the corresponding graph of the gravitational potential force lines for the Eros.

### 3. Motion simulation in an irregular gravitational field for an electric propulsion spacecraft

#### 3.1 Simulation a passive spacecraft's motion

As we have already mentioned, the gravitational potential of the object can be represented as a set of attracting point masses. We will address the gravitational

potential (1) in the inertial Cartesian three-dimensional coordinate system, which begins at the mass center  $B_s$  (**Figure 3**). The axis  $B_sZ$  associates with the axis of asteroid's rotation.

We used the following assumptions to the simulations:

- the asteroid and the spacecraft are moving in the plane  $XB_sY$ , the asteroid rotates clockwise, and the spacecraft rotates counter clockwise;
- the spacecraft has no impact on mass points motions (restricted circular three body problem);
- the Sun's gravity has impacted to the spacecraft and asteroid [17].

Vector form of the differential equations of the disturbed spacecraft's motion is [16]:

$$\frac{d^2\mathbf{r}}{dt^2} = -G \sum_{i=1}^n \frac{M_i}{r_i^3} (\mathbf{r} - \mathbf{r}_i) + \mu_{Sun} \left( \frac{\Delta}{\Delta^3} - \frac{\mathbf{r}}{r^3} \right) + \frac{\mathbf{P}}{m_{SV}}; \quad (3)$$

$$\frac{dm_{SV}}{dt} = -\delta\tau \quad (4)$$

where  $\mathbf{P}$  is controlling thrust vector;  $\tau$  is propellant consumption per second;  $\delta$  is Boolean-function of the engine operating condition (it can be 0 or 1); and  $m_{SV}$  is the spacecraft mass,  $\mu_{Sun}$  is gravity parameter of Sun.

From now on, a radius is in km, velocity is in kilometer per second, thrust is in Newton, and angle is in radians. The integration scheme is the Runge-Kutta method (fourth-order accuracy). It is also noteworthy that all osculating parameters of orbit were obtained in the presumption that the asteroid's mass localizes in barycentre point.

We used the spacecraft's parameters, like to the missions Dawn and Rosetta [18], to simulate motion in these cases. The spacecraft's mass is 1200 kg and the exhaust velocity of the engine is 20 km/s. The initial commencing speed in every case was

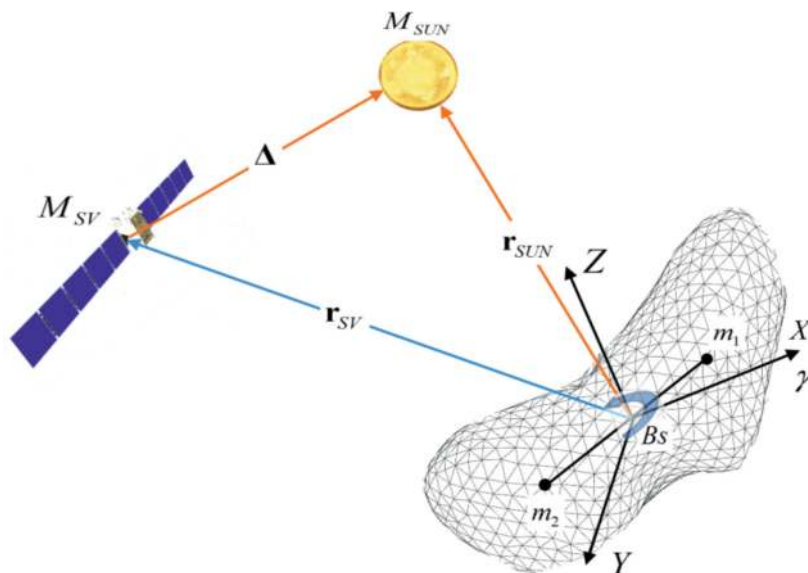


**Figure 3.**  
 Scheme of the three body problem.



chosen close to the circular velocity of the asteroid as the body with only one gravity point. The launch date is May 30, 2018. The authors developed the software for simulating spacecraft motion in irregular and regular gravitational fields [1].

To compare the impact of the distance from asteroid Eros on the spacecraft trajectory, we proposed to perform motion simulation for two orbit altitudes—50 km and 100 km. The same simulation to the asteroid Gaspra was performed for an orbit altitude of 200 km. **Table 2** presents the initial conditions for the three cases.

**Figures 4** and **5** illustrate the trajectories of the passive spacecraft motion for two orbit altitudes in the plane: 50 km and 100 km from asteroid Eros. According to the graphs, orbits are not stable; moreover, in the first case, the spacecraft hits the asteroid after 18.35 days.

### 3.2 Simulation controlled spacecraft’s motion: locally optimal controlled law

One of the problems of controlled spacecraft motion simulation is to find simple schemes to control the spacecraft that allow performing some simple maneuvers or stabilizing an orbit.

Case	r, km	V, km/s
Eros1	50	$2.98 \times 10^{-3}$
Eros2	100	$2.1 \times 10^{-3}$
Gaspra1	100	$2.76 \times 10^{-3}$

**Table 2.**  
Initial conditions for the three cases of simulation.

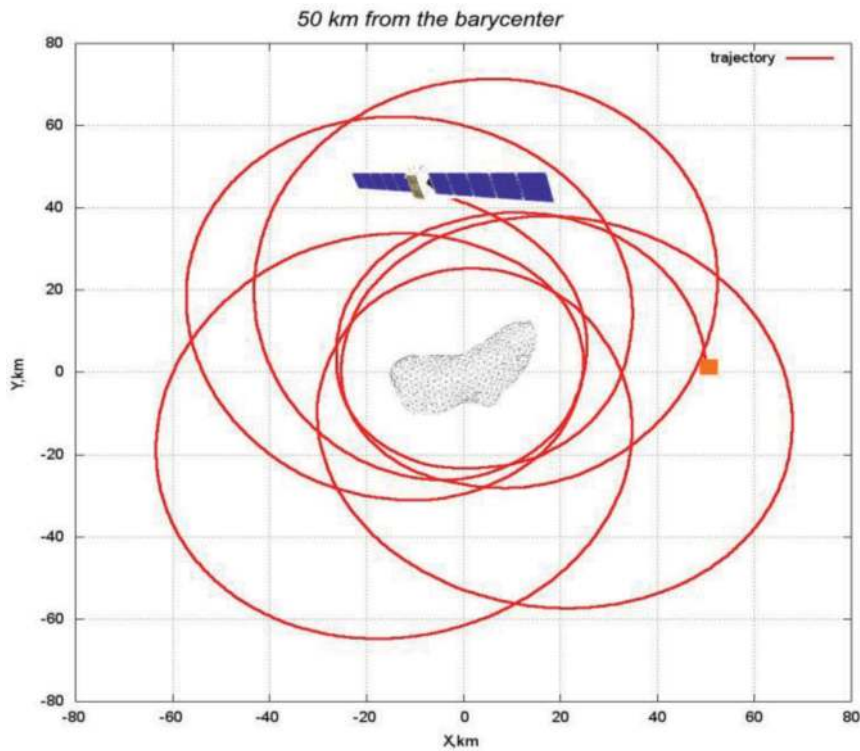


**Figure 4.**  
Trajectory of passive spacecraft motion near the Eros in the plane XB&Y (case Eros1)  
 $r = (0 \ 50 \ 0)^T$ ;  $V = (0 \ 2.98 \cdot 10^{-3} \ 0)^T$ .

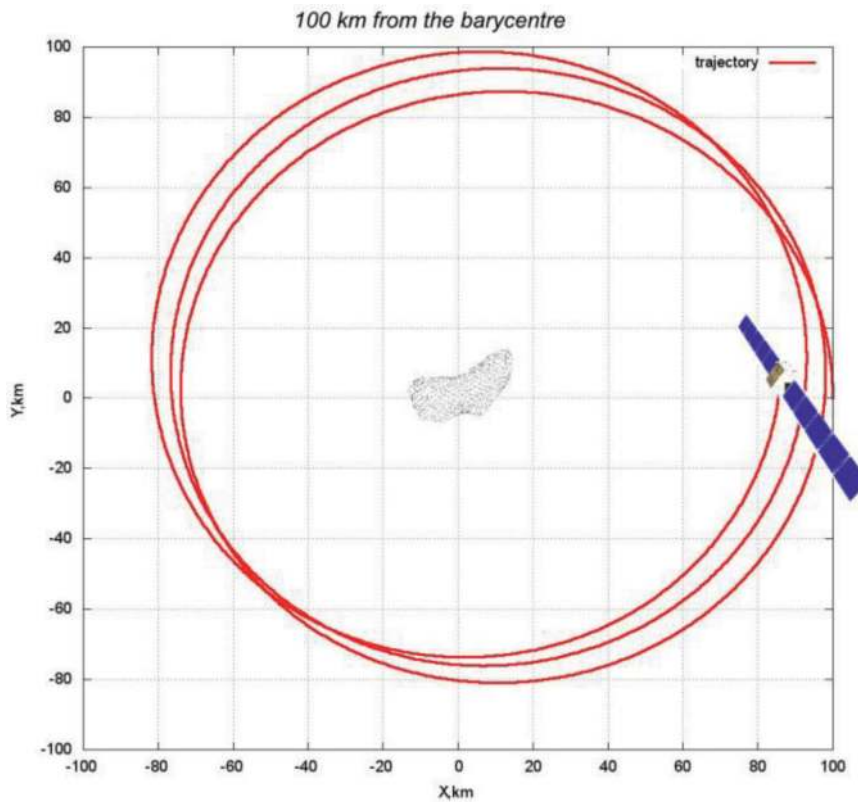


**Figure 5.**

Trajectory of passive spacecraft motion near the Eros in the plane  $XB_sY$  (case Eros2)  $\mathbf{r} = (0 \ 100 \ 0)^T$ ;  
 $\mathbf{V} = (0 \ 2.1 \cdot 10^{-3} \ 0)^T$ .

The primary requirement for these control schemes is the simplicity in operation. Consequently, it is suggested to use locally optimal actions based on osculating orbital elements. A spacecraft is assumed to move along the barycentric orbit, and corresponding osculating elements appertain to this orbit's plane. According to [17], application of the laws based on osculating orbital elements in this particular case allows obtaining a stable orbit for a spacecraft with an electric propulsion engine. It is suggested to use an angle  $\eta$  between the radius vector of the spacecraft  $\mathbf{r}$  and the propulsive force vector  $\mathbf{P}$  (Figure 6).

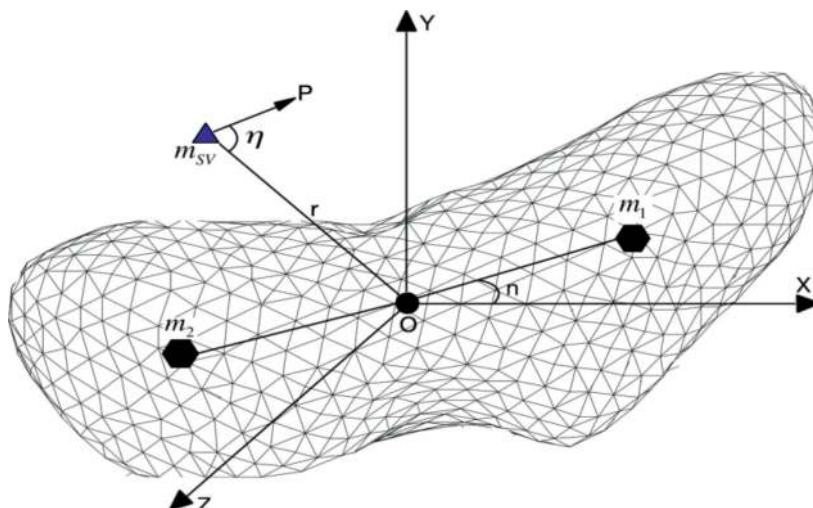


**Figure 6.**

Barycentric rectangular coordinate system—the Eros and the spacecraft appertain to the plane.

The constant semi-major axis law is considered [17] as the control law:

$$\operatorname{tg}\eta = -\frac{e \sin \vartheta}{1 + e \cos \vartheta} \quad (5)$$

where  $\vartheta$  is true anomaly and  $e$  is eccentricity of the barycentric orbit. The equations of the control thrust vector are:

$$P_x = \frac{r_x}{\sqrt{r_x^2 + r_y^2}} \cos \eta - \frac{r_y}{\sqrt{r_x^2 + r_y^2}} \sin \eta \quad (6)$$

$$P_y = \frac{r_y}{\sqrt{r_x^2 + r_y^2}} \cos \eta + \frac{r_x}{\sqrt{r_x^2 + r_y^2}} \sin \eta \quad (7)$$

$$P_z = 0 \quad (8)$$

The simulation parameters were determined earlier. Additionally, the specific impulse of the engine module is  $IsP1 = 1000$  s,  $IsP2 = 1500$  s, and  $IsP3 = 2000$  s. The thrust values are various for the particular altitude. The particular values were obtained by the direct-search method.

The interpolated values of thrust levels for the orbit's stabilization control scheme (16) for  $IsP1 = 1000$  s,  $IsP2 = 1500$  s, and  $IsP3 = 2000$  s are represented in **Figure 7**.

**Figures 8 and 9** show graphs of changes in orbit parameters in case Eros1 and the engines with  $IsP1 = 1500$  s.

**Figure 10** shows the trajectory of spacecraft's motion in the OXY for 50 km Eros' orbit (case Eros1). The characteristic of thrust for the orbit altitude in 50 km and for the orbit altitude of 100 km are shown in **Table 3**.

**Figure 11** shows trajectory of spacecraft's motion in the OXY for 100 km Eros' orbit (case Eros2).

Consider the trajectory of motion for the case of asteroid Gaspra, obtained by using the locally optimal control law—the constancy of the distance of the semi major axis (**Figure 12**), as well as graphs of changes in the barycentric coordinates

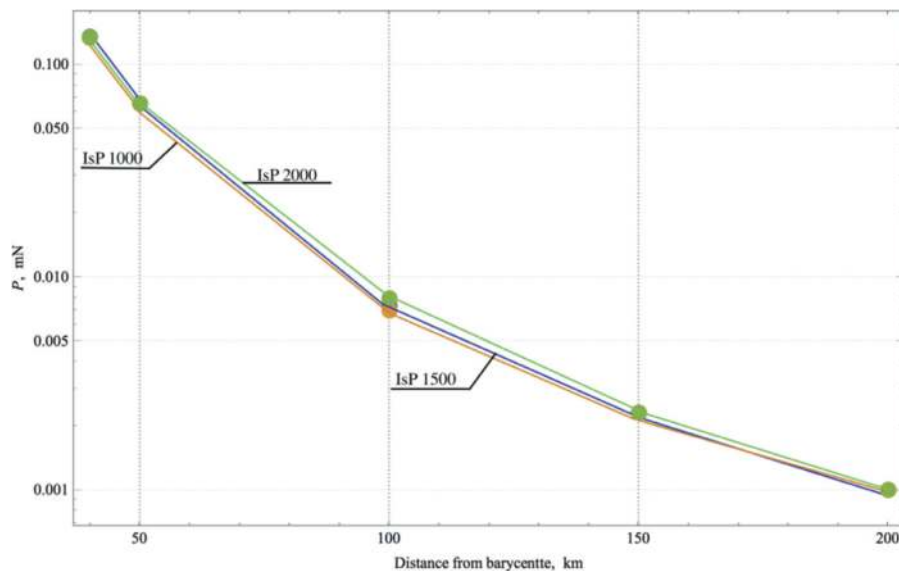


**Figure 7.** Dependency of the thrust level to the barycentre distance and the specific impulse of propulsion system.



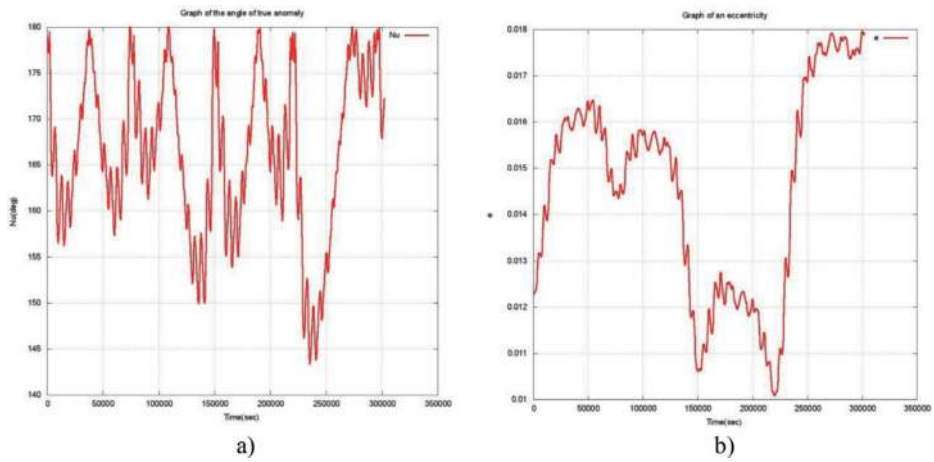


**Figure 8.**  
 Graphs of changes in the parameters of the trajectory (case Eros1). (a) The angle of the true anomaly and (b) eccentricity.

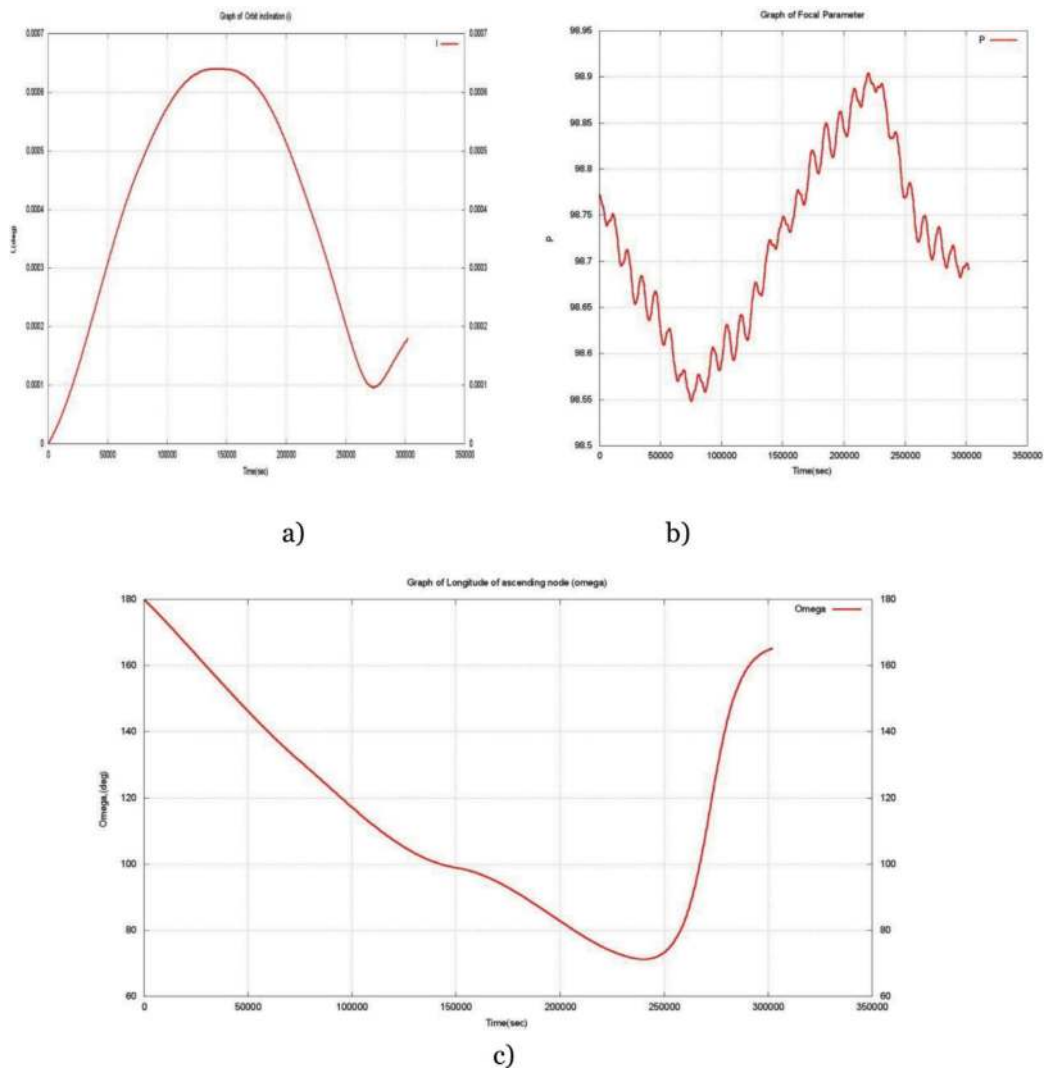


**Figure 9.**  
 Graphs of changes in the parameters of the trajectory (case Eros1). (a) Focal parameter, (b) inclination, and (c) longitude of the ascending node.

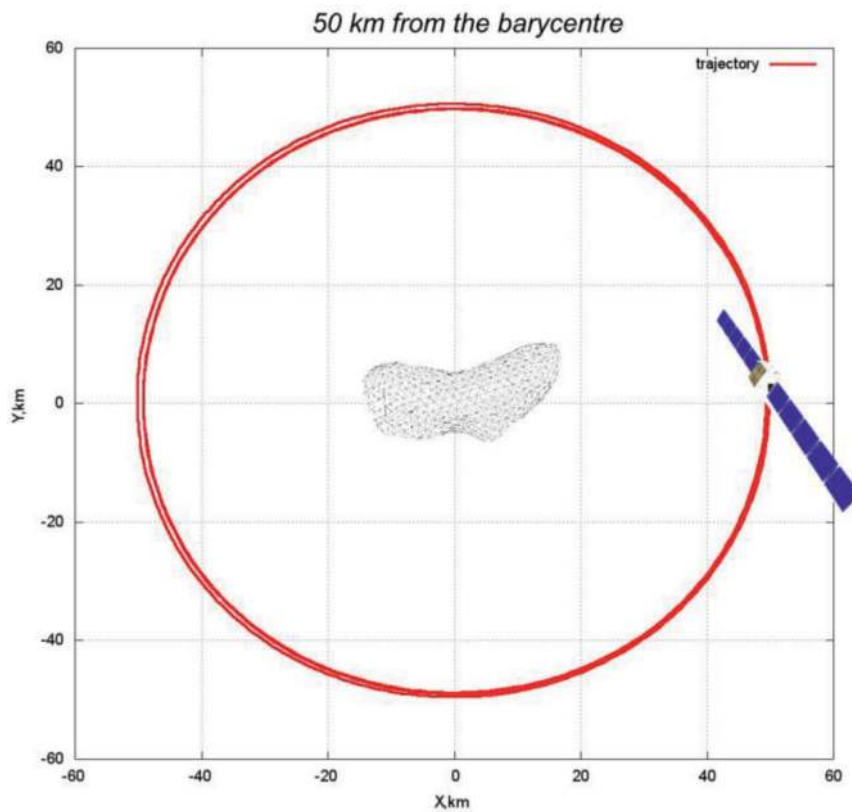


**Figure 10.**  
Trajectory of spacecraft's motion near the Eros stabilized by the constant semi-major axis law  
 $r = (0 \ 50 \ 0)^T$ ;  $V = (0 \ 2.98 \cdot 10^{-3} \ 0)^T$ ,  $P = 6.6 \cdot 10^{-5} N$  (case Eros1).

Case	r, km	P, N	c, km/s
Eros1	50	$6.6 \times 10^{-5}$	15
Eros2	100	$8 \times 10^{-6}$	15
Gaspra1	100	$2.33 \times 10^{-5}$	20

**Table 3.**  
Characteristics of thrust and exhaust velocity.

and velocities of the spacecraft (Figures 13 and 14) and graphs of changes in the orbit parameters (Figures 15 and 16).

#### 4. Ion electrospay thruster assembly for spacecraft maneuvering in vicinity of asteroid

Ion electrospay engine (iESP) is a micro-thruster that is designed initially for CubeSats technology. Besides, such engines can be used for motion control systems of small spacecraft as these engines have a sufficient duration of operation and low consumption of the working fluid. It is a type of low thrust electric propulsion rocket engine that uses electrostatic acceleration of charged liquid droplets for propulsion. The liquid used for this application tends to be a low-volatility ionic liquid. The most amenable propellants for electrostatic thrusters have proven to be

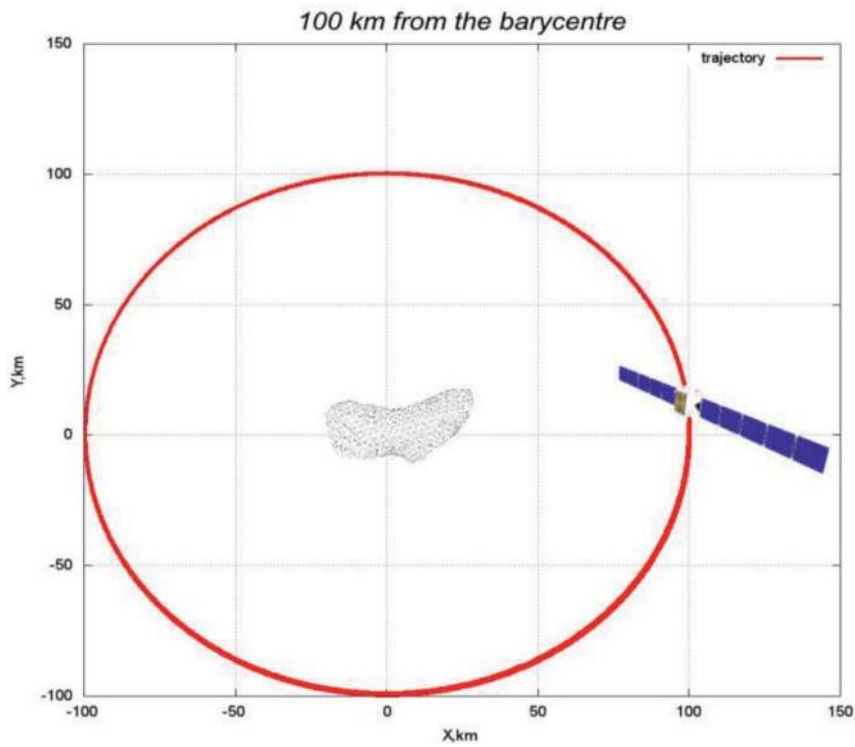


**Figure 11.**  
 Trajectory of spacecraft's motion near the Eros stabilized by the constant semi-major axis law  
 $r = (0 \ 100 \ 0)^T$ ;  $V = (0 \ 2.1 \cdot 10^{-3} \ 0)^T$ ,  $P = 8 \cdot 10^{-6} N$  (case Eros2).

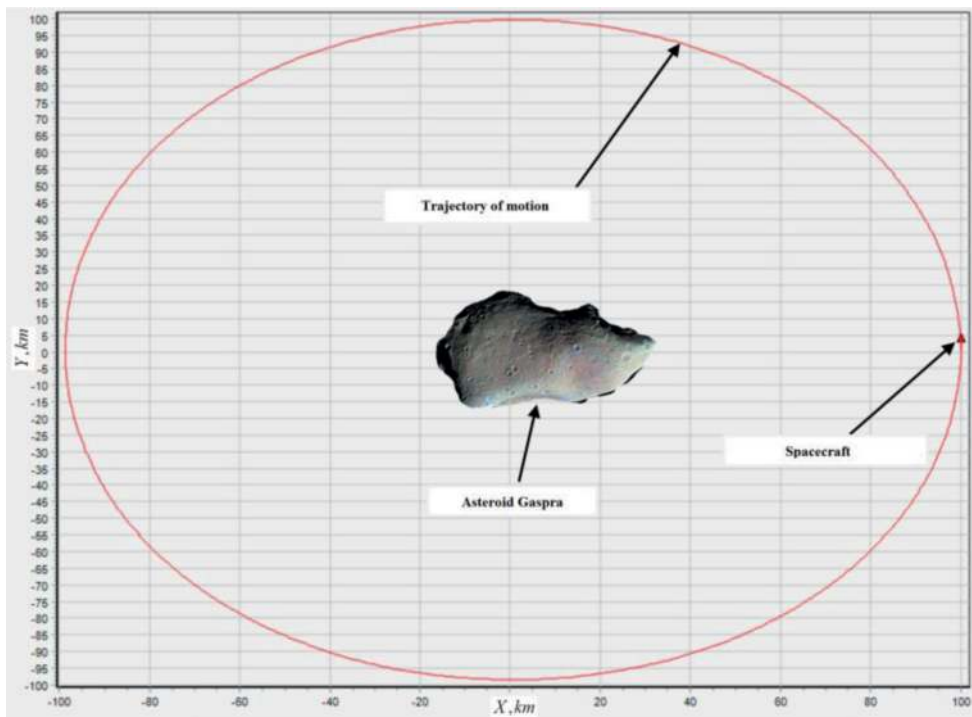


**Figure 12.**  
 The trajectory of the spacecraft for asteroid Gaspra (case Gaspra1).

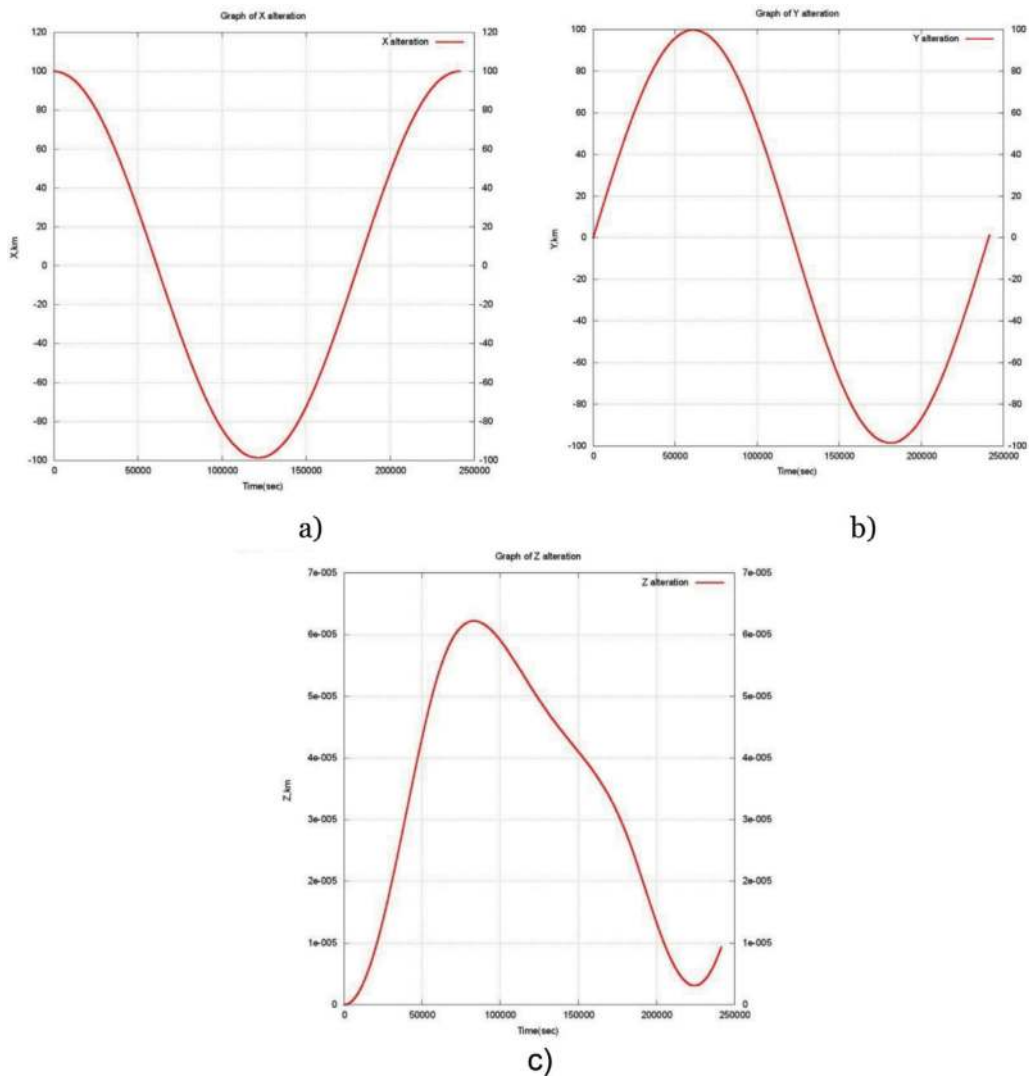


**Figure 13.** Graphs of changes in the parameters of the trajectory (case Gaspra1). (a) X coordinate, (b) the Y coordinates, and (c) Z coordinates.

cesium, mercury, argon, krypton, and most commonly xenon, and many possible sources of such ions of the requisite efficiency, reliability, and uniformity have been conceived and developed [19].

The typical design appearances of an electrospay thruster are shown **Figures 17** and **18**.

Like other ion thrusters, the main benefits of iESP include high efficiency, thrust density, and specific impulse; however, it has shallow total thrust, on the order of micro-Newton. It provides excellent attitude control or dynamic acceleration of small spacecraft over long periods.

The spacecraft's motion simulation in asteroid's vicinity identifies that engine specification for the stabilization trajectories is close to the Ion electrospay thrusters' modules in the context of the thrust level and  $I_{sp}$ . Therefore, we propose to use them not only as executive bodies of the control system, but also to stabilize the orbital motion of the spacecraft, which is unstable due to the disturbing action of an irregular gravitational field. The appearance of the control program identifies the number of demands for the electrospay engines module that is installed on the spacecraft. It can be used for the particular configuration of the power plant's design.

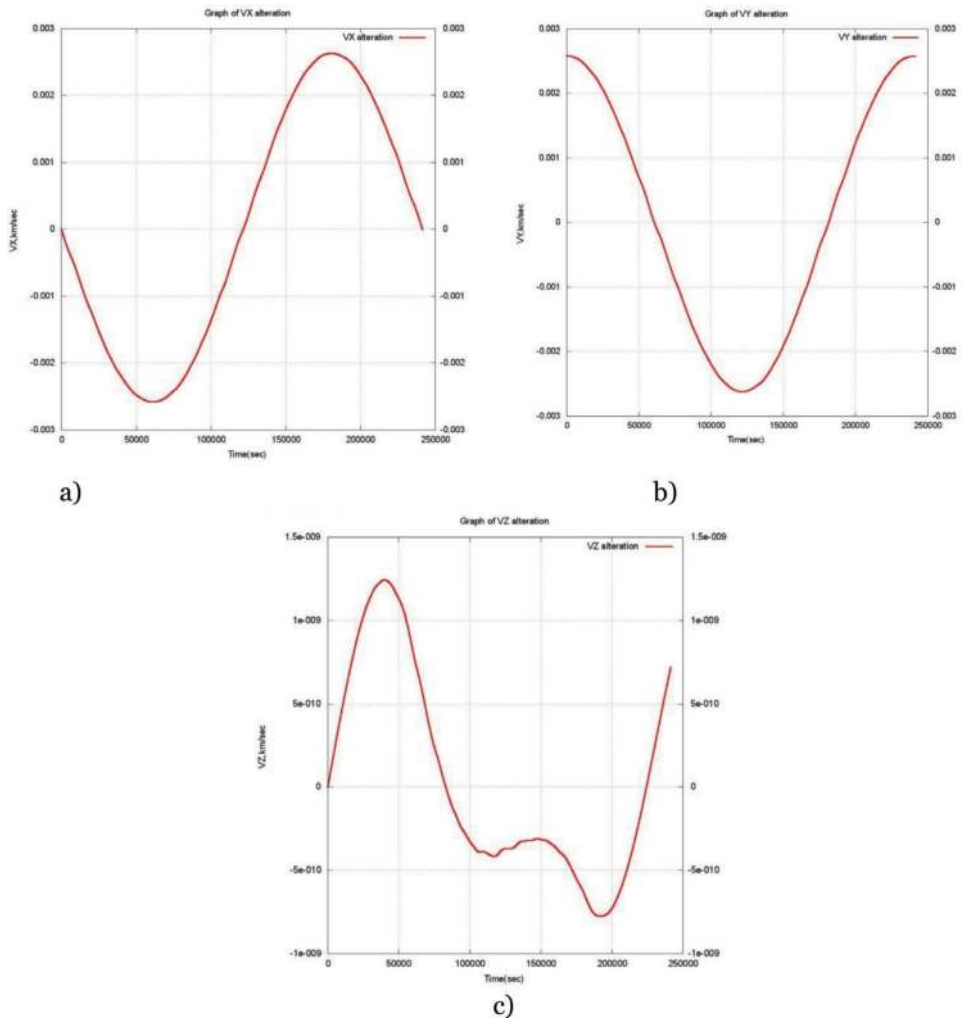


**Figure 14.** Graphs of changes in the parameters of the trajectory (case Gaspra1). (a) Vx velocity, (b) Vy velocity, and (c) Vz velocity.

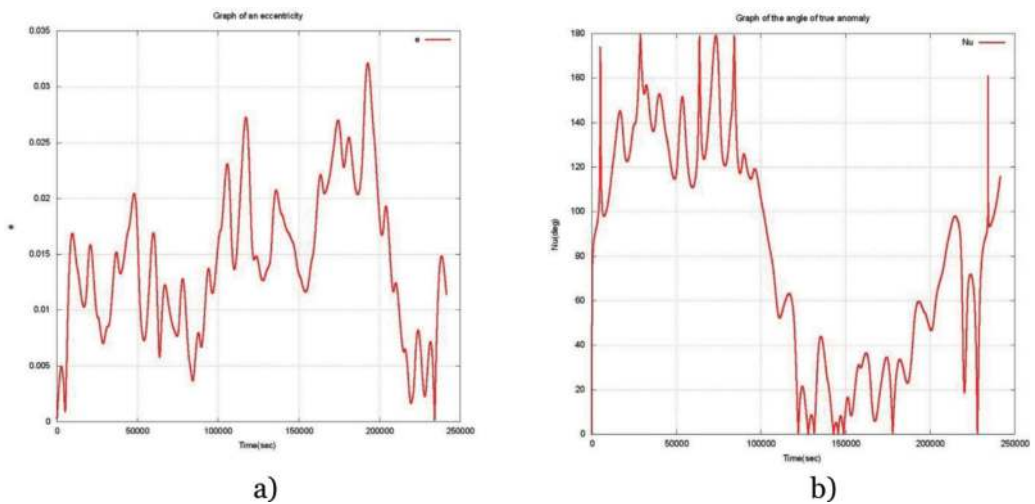


**Figure 15.** Graphs of changes in the parameters of the trajectory (case Gaspra1). (a) The eccentricity and (b) the angle of the true anomaly.



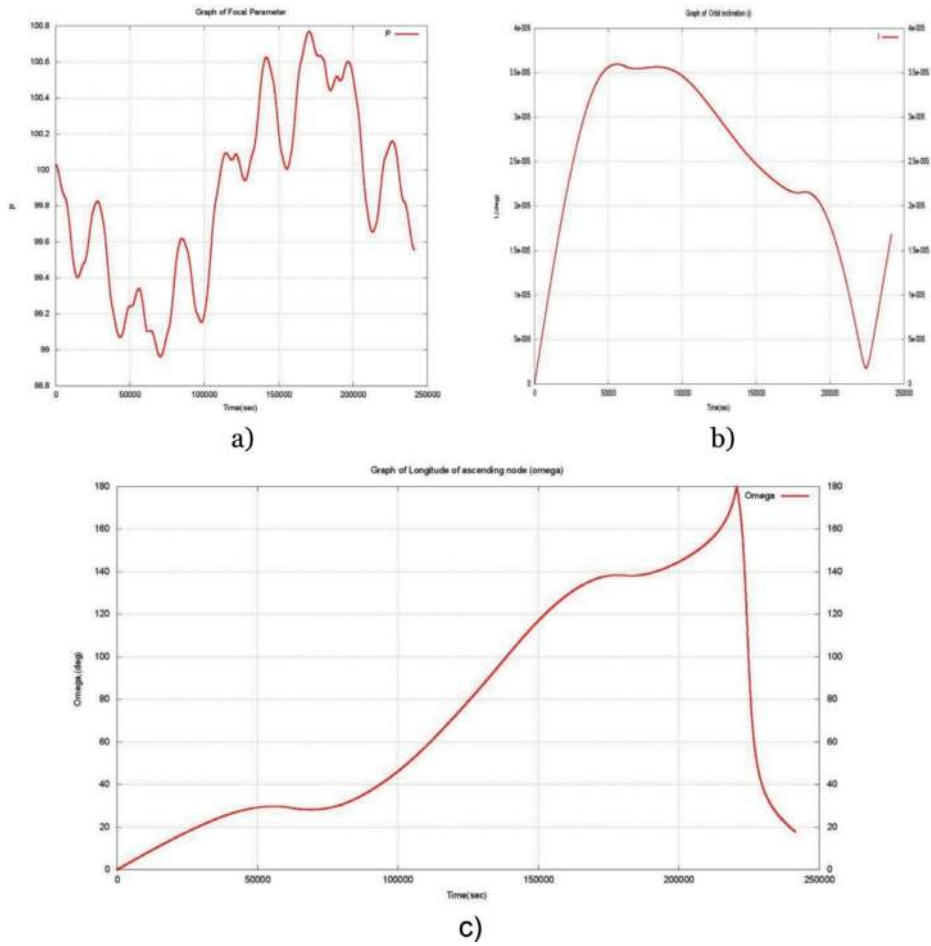


**Figure 16.** Graphs of changes in the parameters of the trajectory (case Gaspra1). (a) Focal parameter, (b) inclination, and (c) longitude of the ascending node.



**Figure 17.** Electro-spray thruster.



**Figure 18.**  
*Electric engine.*

**Figures 19–21** show diagrams of the control law for the cases Eros1, Eros2, and Gaspra1 (control programs). It can be seen from the graphs that small changes in the direction of thrust of the engine (within  $10^\circ$ ), according to the selected control law, allows making the flight orbits stable. Such control rules can be used to maneuver near an asteroid with an uneven gravitational field.

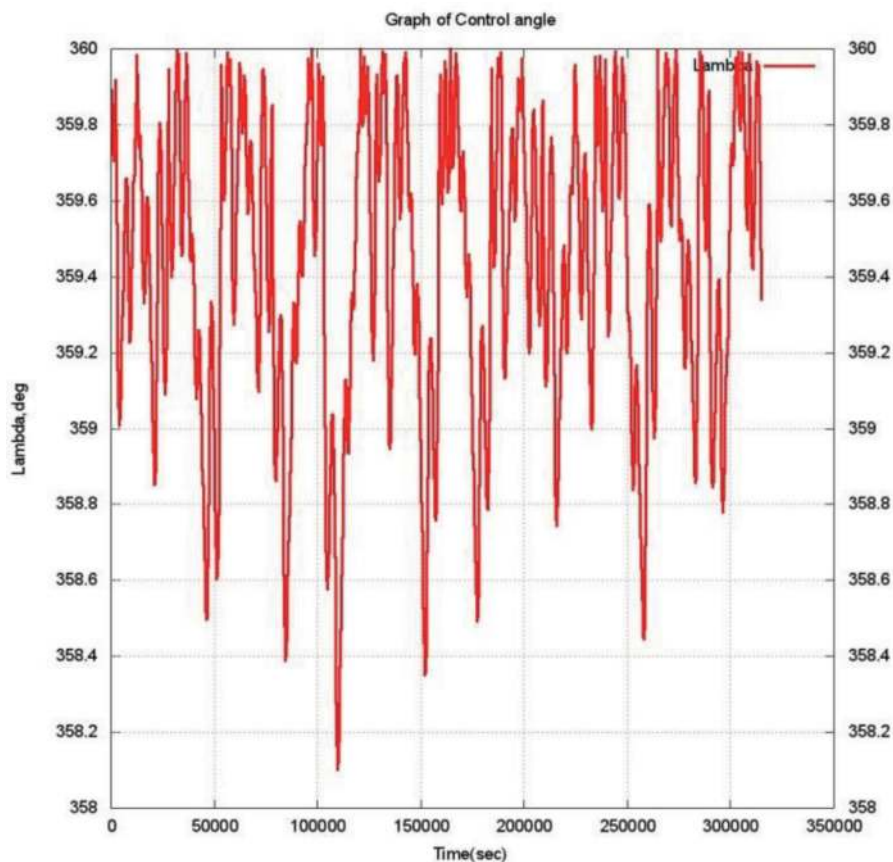


**Figure 19.**  
*The control program for the constant semi-major axis (50 km) (case Eros1).*

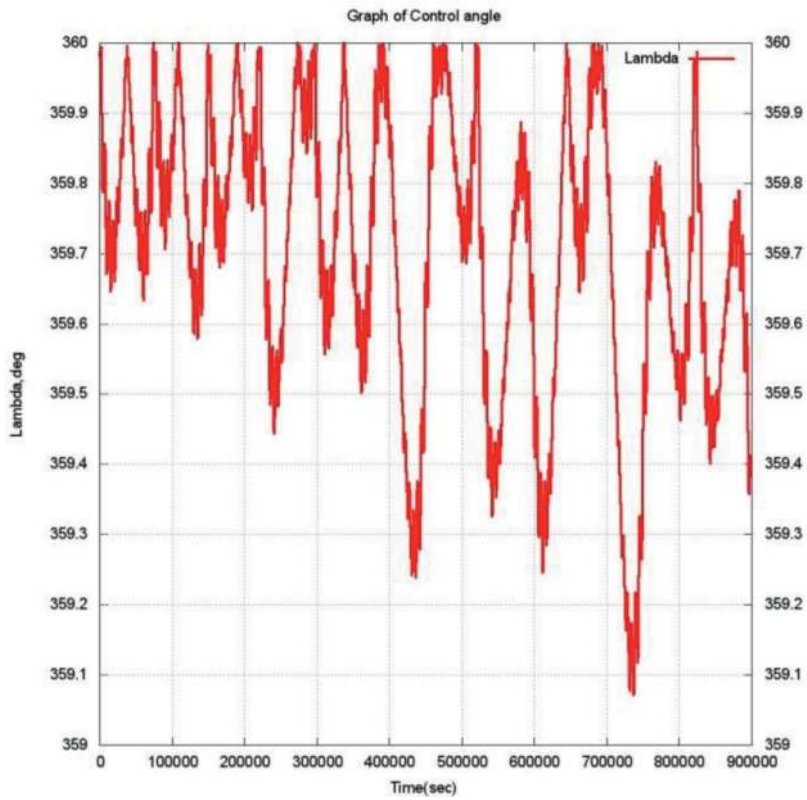


**Figure 20.**  
*The control program for the constant semi-major axis (100 km) (case Eros2).*

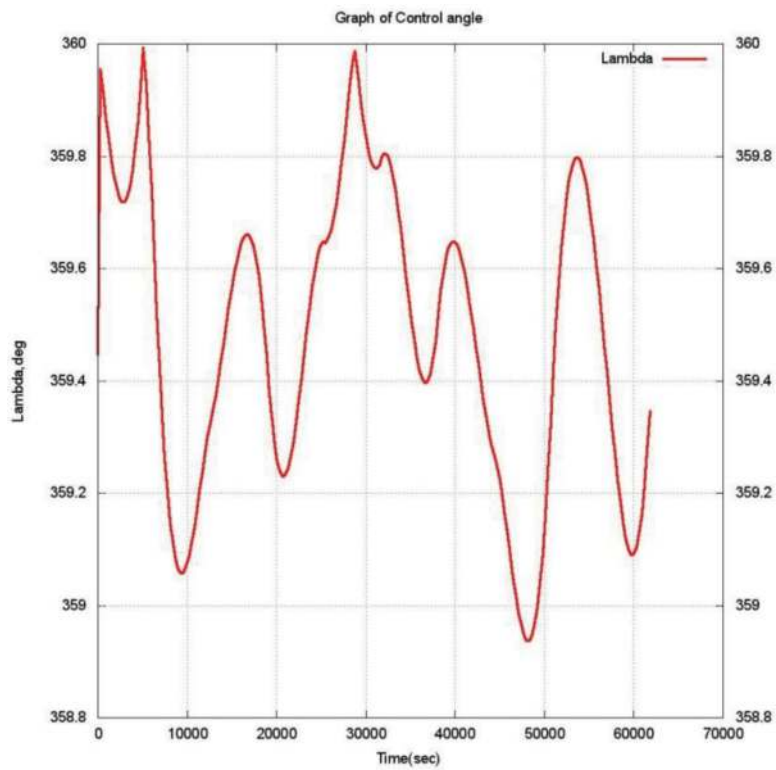


**Figure 21.**  
*The control program for the constant semi-major axis (100 km) (case Gaspra1).*

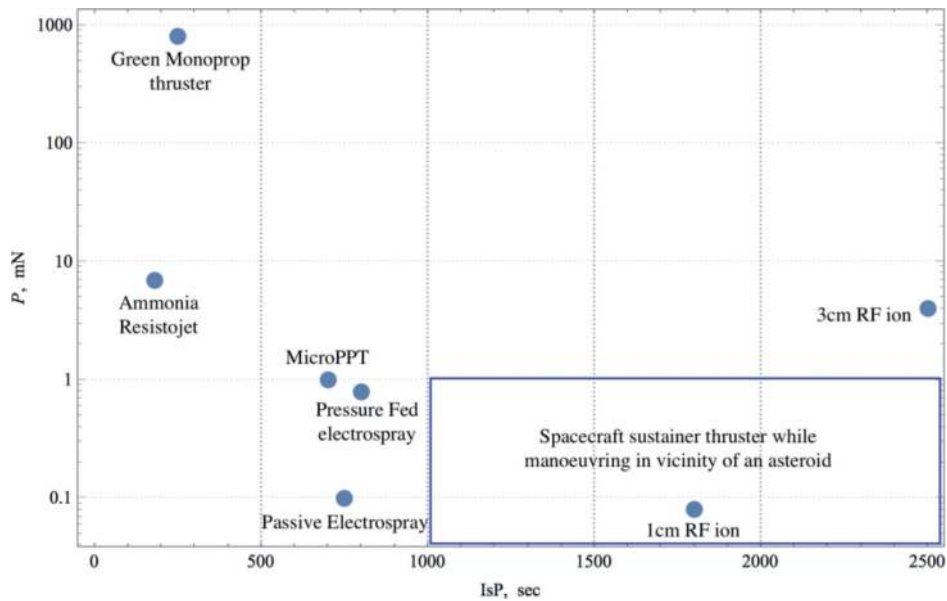


**Figure 22.**  
*Electric engine thrust/IsP distribution for suitable electric propulsion systems.*

Thus, iESP modules can be successfully used not only for the control angular motion, but also for the movement in the vicinity of an asteroid in different research missions.

The simulation results of the orbital stabilization for other engines (for other specific impulse and thrust values) and orbit altitudes were not represented in the chapter; however, the obtained values were used for interpolation lines (**Figure 6**). Thrust levels were variable parameters that depend on the orbit altitude and the initial commencing speed. **Figure 22** shows the range of settings of electric propulsion systems suitable for use as an engine for maneuvering or stabilizing near-asteroid orbits.

## 5. Conclusions

This chapter discusses the use of electro spray engines to stabilize near-asteroid orbits. Presents two of the asteroids Eros and Gaspra have substantially nonspherical. Mathematical models of the asteroid's gravitational field and controlled motion of a spacecraft with an electric motor in an uneven gravitational field are developed.

The obtained results are used to simulate the passive and controlled motion of a spacecraft as an n-body problem. It is established that passive motion is unstable. The authors proposed to use the known locally optimal control law for orbit stabilization. A constant semi-axis control law of thrust was used to model the motion of three orbits (50, 100, and 200 km) near two asteroids (Eros and Gaspra) to stabilize. The levels of thrust and specific impulse and their dependence on the orbit height, initial velocity, and asteroid parameters were determined.

The simulation results show that the calculated thrust and specific impulse (or exhaust velocity) levels are within the range of ion motor characteristics. However, it is necessary to take into account the received control programs and the real and mass of the spacecraft. Therefore, under all these assumptions, it is possible to use the ion electro spray module for motion near asteroids.

The simulation results show that the calculated thrust and exhaust velocity levels are too low for the spacecraft's main engines. Thus, to guarantee the design characteristics, it is necessary to use an additional module iESP.

## **Acknowledgements**

The authors state that part of the chapter was taken from our previously published article (Andrey Shornikov, Irina Gorbunova, Olga Starinova "Stabilized Trajectories of a Spacecraft in Inhomogeneous Gravitational Fields," AIP Publishing, 2018), and that we have the copyright to re-use it. The reported study was funded by Ministry of Education and Science of the Russian Federation according to the research project No. AAAA-A17-117031050032-9 (9.5453.2017).

## **Author details**

Olga Starinova<sup>1</sup>, Andrey Shornikov<sup>1</sup> and Elizaveta Nikolaeva<sup>2\*</sup>


1 Department of Space Engineering, Samara National Research University, Samara, Russia

2 Interuniversity Department of Space Research, Samara National Research University, Samara, Russia

\*Address all correspondence to: nikolaevalizaveta@mail.ru

## **IntechOpen**

---

© 2019 The Author(s). Licensee IntechOpen. This chapter is distributed under the terms of the Creative Commons Attribution License (<http://creativecommons.org/licenses/by/3.0>), which permits unrestricted use, distribution, and reproduction in any medium, provided the original work is properly cited. 



## References

- [1] Shornikov A, Starinova O. Effectiveness analyses of an electro-spray sustainer engine installed on a spacecraft maneuvering in vicinity of an asteroid. *Procedia Engineering*. 2017
- [2] Chapman CR, Morrison D. On the Earth by asteroids and comet: Assessing the hazard. *Nature*. 1994;**367**:6458, 33-6440
- [3] Ross SD. Near-Earth asteroid mining space. Use of near-Earth asteroids as platforms for future space bases; 2001
- [4] Moore S. Technology development for NASA's asteroid redirect
- [5] Britt DT et al. Asteroid density, porosity, and structure. In: *Asteroids III*. 1987
- [6] Geissler P, Petit J-M, Durda D, Greenberg R, Bottke W, Nolan M, et al. *Icarus*. 1996;**120**:140
- [7] Ren Y, Shan J. On tethered sample and mooring systems near irregular asteroids. *Advances in Space Research*. 2014;**54**(8):1608-1618
- [8] Hu X, Jekeli C. A numerical comparison of spherical, spheroidal and ellipsoidal harmonic gravitational field models for small non-spherical bodies: Examples for the Martian moons. *Journal of Geodesy*. 2015;**89**(2):159-177
- [9] Wang X, Jiang Y, Gong S. Analysis of the potential field and equilibrium points of irregular-shaped minor celestial bodies. *Astrophysics and Space Science*. 2014;**353**(1):105-121
- [10] Michel P, Farinella P, Froeschlé C. The orbital evolution of the asteroid Eros and implications for collision with the Earth. *Nature*. 1996;**380**(6576):689
- [11] Garmier R et al. Modeling of the Eros gravity field as is ellipsoidal harmonic expansion from the near Doppler track data. *Geophysical Research Letters*. 2002;**29**(8)
- [12] Miller JK et al. Determination of shape, gravity, and rotational state of asteroid 433 Eros. *Icarus*. 2002;**155**(1): 3-17
- [13] Moore C. Technology Development for NASA's Asteroid Redirect Mission, IAC-14-D2.8-A5.4.1. Available from: [https://www.nasa.gov/sites/default/files/iles/IAC-14-D2\\_8-A5\\_4\\_1-Moore.pdf](https://www.nasa.gov/sites/default/files/iles/IAC-14-D2_8-A5_4_1-Moore.pdf)
- [14] Asteroids internet base. Available from: <http://space.frieger.com/asteroids/>
- [15] Shornikov A, Starinova O. Simulation of controlled motion in an irregular gravitational field for an electric propulsion spacecraft. In: *Proceedings of the IEEE 7th International Conference on Recent Advances in Space Technologies (RAST)*; 16–19 June 2015; Istanbul, Turkey. 2015. pp. 771-776
- [16] Szebehely V. *Theory of Orbits: The Restricted Problem of Three Bodies*. New Haven, CT: Yale University; 1967. pp. 10-25
- [17] Lebedev V. *The Calculation of the Motion of a Spacecraft with Low Thrust*. Moscow: Computation Centre of the Russian Academy of Sciences; 1968. pp. 4-10
- [18] Scheeres D. The orbital dynamics environment of 433 Eros. *Ann Arbor*. 2002. 1001
- [19] Sheth V. Spacecraft electric propulsion—A review. *International Journal of Research in Aeronautical and Mechanical Engineering*. 2014;43-55. ISSN: 2321-3051